5th Multiphase Flow Journeys
May 17th-18th, 2019, Rio de Janeiro, RJ, Brazil

JEM-2019-XXXX
HYDRODYNAMICS OF AN AIR-WATER SLUG FLOW RISING THROUGH STAGNANT LIQUIDS

Izabela V. dos Santos
Antônio G. B. da Cruz
Marcelo O. Silva
Faculty of Mechanical Engineering, ITEC, Federal University of Pará, Belém, Brazil
izabela_vs@hotmail.com
aguicruz@ufpa.br
mos@ufpa.br

Abstract. *An experimental and numerical study on the hydrodynamics of air-water slug flow in vertical column stagnant liquid is presented in this paper. A fast film technique is applied to obtain parameters of the flow of a single bubble rising stagnant water under laminar flow inside a circular tube for different entry volumes of air, including the rising velocity, bubble length, and liquid film thickness. The numerical study is based on the phase field model solving the momentum and Cahn-Hilliard equations. The phase field model was applied to simulate flows with the same characteristics as the experimental ones, as well as extrapolate it to study flow conditions that are not easily possible in an experimental approach. Due to the lack of experimental data on flows with high values of N_f, simulations will be extended to cover different column diameters and Eötvös numbers.*

Keywords: *slug flow, liquid film, Taylor bubble, phase-field*

1. INTRODUCTION

The slug flow pattern is characterized by elongated gas bubbles that occupy nearly the entire diameter of the tube, these bubbles, also known as Taylor bubbles, generally, have a longer length than the radius of the tube and are characterized by a flat tail and a molded front. The Taylor bubbles separate themselves from the pipe wall by a thin film of liquid which flows in the opposite direction of the bubble. At the end of the bubble, this film separates itself from the bubble creating a wake that may or may not have turbulent character (de Oliveira *et al.*, 2015).

The liquid film region, according to Brown (1965), can be divided into two others regions: one near the top of the bubble in which one part of the liquid accelerates by the effect of gravity and the other is supported by the shear stress in the wall and a second region, where all the liquid is supported by the shear stress. In this second region, the liquid film is considered totally developed and has a constant thickness δ which is according to Thome *et al.* (2004), of fundamental importance for the development of heat transfer models for two-phase flows.

The hydrodynamics of a taylor bubble rising through stagnant liquid is governed by the interaction between gravitational, viscous, interfacial and inertial forces. Neglecting the effects of the expansion of the gas bubble during its rise, we use the Pi-Buckingham theorem to perform a dimensional analysis and the problem can be reduced to three dimensionless groupsAraújo *et al.* (2012).

The Froud number $\left(Fr = \frac{U_{TB}^2 \rho_L}{gD(\rho_L - \rho_G}\right)$ that is the ratio of inertial and gravitational forces.

The Eötvös group $\left(Eo = \frac{g(\rho_L - \rho_G)D^2}{\sigma}\right)$, which is defined by the ratio of the surface tension and the gravitational forces.

The Morton group $\left(M = \frac{g\mu_L^4(\rho_L - \rho_G)}{\rho_L^2 \sigma^3}\right)$ that contains the properties of the fluids.

Derived from the Eötvös group and Morton group is the inverse viscosity number ($N_f = (Eo/M)^{1/4}$, where ρ_L and ρ_G are the densities of the liquid and the gas phase, respectively, μ_L is the dynamic viscosity of the liquid phase, D is the tube diameter, σ is the surface tension between phases and U_{TB} is the Taylor bubble rising velocity.

In this paper, we study the hydrodynamics of a single Taylor bubble in vertical slug flow using a phase field method solving the Navier-Stokes and Cahn-Hilliard bulk equations. An experiment is carried out using a fast filming technique to obtain parameters of the flow of a single bubble rising in stagnant liquid, including the rising velocity, bubble length and liquid film thickness in a circular tube of 25.4 mm in diameter for different volumes of gas. Then, a numerical study is applied to simulate flows with the same characteristics as the experimental ones as well as more complex flows in which

the experimental approach used is not as efficient. Due to the lack of experimental data on flows with high numbers of N_f and on the hydrodynamics of the annular region of the liquid film (Morgado *et al.*, 2016), simulations will be extended to cover different column diameters, Eötvös numbers, and a particular interest will be taken in this region.

2. EXPERIMENTAL APPROACH

We use the fast filming technique to obtain the velocity, length of the Taylor bubble, and the thickness of the liquid film region. The scheme of the experimental apparatus is shown in Figure 1.

The experiment consists of a tube filled with stagnant water in which controlled volumes of air are injected into the base of the tube to form the desired slug flow pattern. The acrylic box delimiting the test section is positioned at a specific distance from the base of the tube and filled with distilled water. A ruler is placed inside the box and used as a reference scale for the measurements obtained by the video camera. The videos are recorded at a rate of 120 frames per second, generating images that will be later processed using the free software *VirtualDub* and *ImageJ* to obtain the parameters of the flow.

The cylindrical acrylic tube with dimensions of 1 m in height, an internal diameter of 25.4 mm and a wall thickness of 2 mm was positioned vertically on a vertical wooden base by metal clamps and with the aid of an inclinometer, it was verified that the tube was 90 from the ground. The tube was then filled with water, forming a column of stagnant liquid.

A transparent acrylic box was placed around the column at a height of 0.4 m from the base of the tube and filled by a solution of distilled water to correct the curvature effects generated by the pipe wall, obtaining thus a flat view of the cylinder and the flow. Inside the box was placed a ruler of 30 cm as a reference scale to assist in the quantitative determination of the characteristics of the bubble. At the same height of the box, was positioned a video camera of the Casio Exilim brand that was programmed to generate videos at an acquisition rate of 120 frames per second.

Air was injected at the base of the water column through a syringe with controlled gas inlet volumes, in the values of 20 ml, 30 ml, and 40 ml. Where 10 measurements were taken for each volume, then 10 videos were generated.

The experiment was carried out in a medium temperature environment of 25C and consists of the generation of bubbles through the injection of gas at the base of the stagnant liquid column, forming bubbles called Taylor bubbles, constituting the flow known as the slug flow. When the bubble passes through the acrylic box, that is, the test section, the camera captures the behavior of the bubble so that proper image treatments are performed to obtain the flow parameters.

3. NUMERICAL METHOD

We consider a phase-field model and its numerical approximation for two-phase incompressible flows.

Here, the hydrodynamics of two-phase flow are governed by the equation for continuity and incompressible momentum equations:

$$\begin{aligned} &\rho\frac{\partial(\mathbf{u})}{\partial t} + \rho\mathbf{u}\cdot\nabla\mathbf{u} = \nabla\cdot\left[-p\mathbf{I} + \mu(\nabla\mathbf{u} + (\nabla\mathbf{u})^{\top}\right] - \rho\mathbf{g} + \mathbf{F_{st}}, \\ &\nabla\cdot\mathbf{u} = 0, \end{aligned} \tag{1}$$

and the Cahn-Hilliard equation for the phase field approach:

$$\begin{aligned} &\frac{\partial\phi}{\partial t} + \mathbf{u}\cdot\nabla\phi = \nabla\cdot\frac{\gamma\lambda}{\epsilon_{pf}^2}\nabla\psi, \\ &\psi = -\nabla\cdot\epsilon_{pf}^2\nabla\phi + (\phi^2-1)\phi + \left(\frac{\epsilon_{pf}^2}{\lambda}\right)\frac{\partial f}{\partial\phi}, \end{aligned} \tag{2}$$

where the σ is the surface tension between phases, $\rho\mathbf{g}$ represents the gravitational force, $\mathbf{F_{st}} = \psi\cdot\nabla\phi$ is the effect of surface tension modeled as a body force, $\lambda = 3\epsilon_{pf}\sigma/\sqrt{8}$ is the magnitude of mixing energy, ϵ_{pf} is the thickness of the interface, $\gamma = \chi\epsilon_{pf}^2$ is the mobilty paramater and χ is the mobility tuning parameter.

This model is implemented using the commercial code COMSOL Multiphysics, which is based on the finite-element method.The computational domain is shown in Figure 1. A pressure-based outflow boundary condition was specified at the channel outlet. At the channel wall and the channel inlet, a wetted wall condition was specified with the contact angle set to $\theta = 150°$.

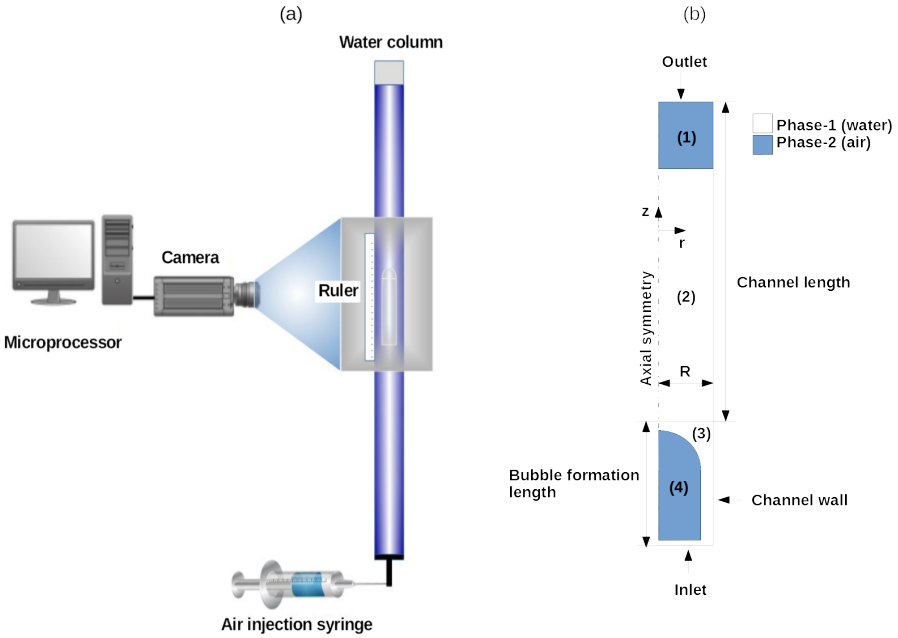

Figure 1: Schematic (a) experimental apparatus and (b) computational domain.

4. RESULTS AND DISCUSSION

We found the lengths and rising velocities of the Taylor bubbles for three sets of air volume: 20 ml, 30 ml, and 40 ml, both experimentally and numerically. The bubble lengths increased with the air volumes and the velocities were the same in all three cases. The shape of the Taylor bubbles found for each volume of air is shown in Fig. 2.

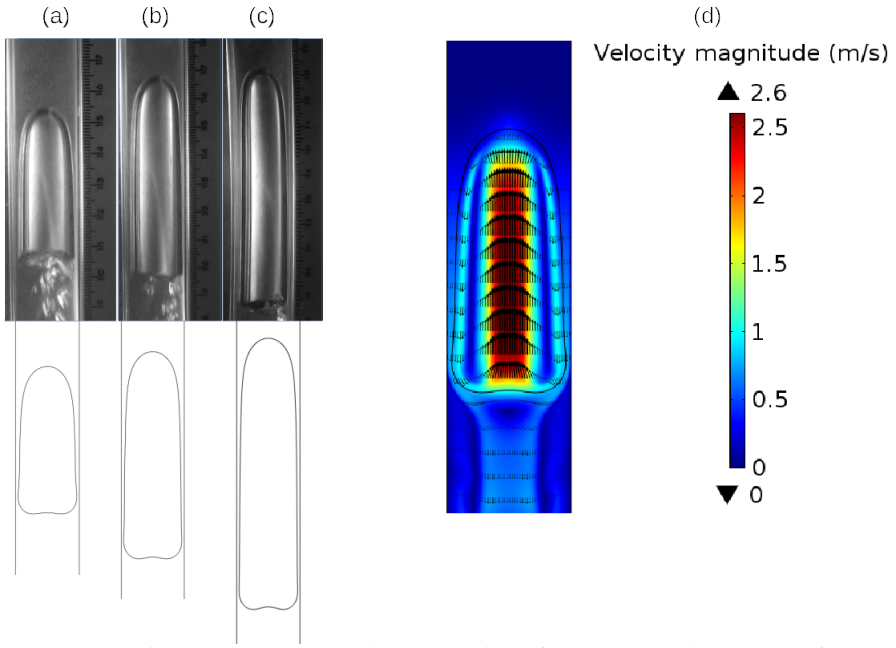

Figure 2: Taylor bubbles experimentally and numerically obtained for the entry air volume of (a) 20 ml, (b) 30 ml and (c) 40 ml and (d) numerical velocity magnitude of a 20ml bubble.

In Table 1 are the experimental and numerical results for the liquid film thickness, Taylor bubble velocity and length. The bubble length and velocity maintain a good agreement between experimental and numerical results, not exceeding 5% of deviation. Fig. 2 shows a comparison between bubble shapes obtained experimentally (top) and numerically (bottom) and it's possible to notice the consistent shape of the bubble's nose and bubble's length for each entry volume of air. It also shows the numerical velocity magnitude of a 20ml bubble and the velocity profile across the radius of the channel.

In the case of liquid film thickness, there is a deviation of up to 35% between the numerical and experimental results shown on 1, but this can be explained by the lack of precision of the experimental technique for the measurement of this

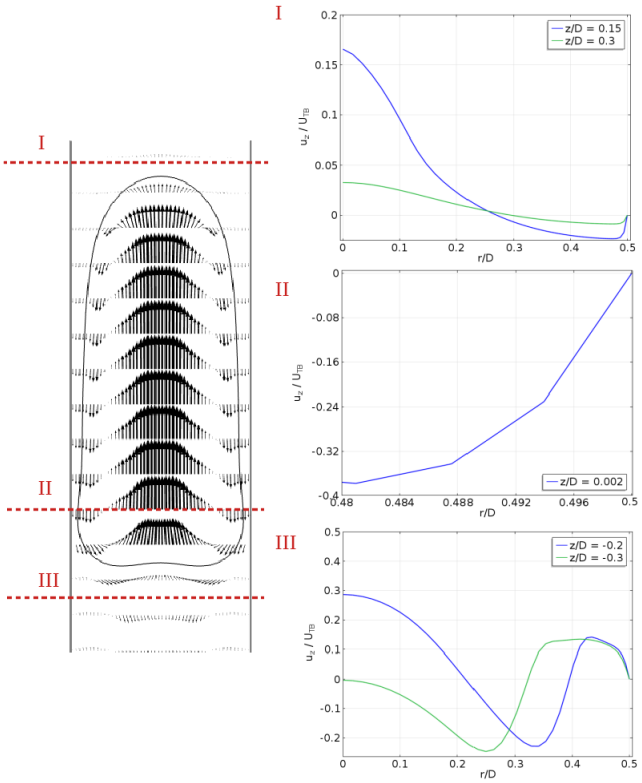

Figure 3: Numerical dimensionless axial velocity profile (u_z/U_{TB}) of the 20ml bubble in a fixed frame of reference (FFR) for different axial iso-surfaces in three regions: above the nose (upper right), developed liquid film (middle right) and on the wake region (bottom right). Representation inspired in Araújo *et al.* (2012).

specific parameter.

Table 1: Experimental and numerical results.

Air volume (ml)	L_{TB}^{exp} **(mm)**	**Err**^{exp} 95%	L_{TB}^{num} **(mm)**	U_{TB}^{exp} **(m/s)**	**Err**^{exp} 95%	U_{TB}^{num} **(m/s)**	δ^{exp} **(mm)**	**Err**^{exp} 95%	δ^{num} **(mm)**
20	47.70	0.80	46.56	0.172	0.02	0.167	2.141	0.103	2.788
30	70.03	1.19	69.01	0.175	0.02	0.172	1.948	0.102	2.629
40	96.57	1.23	93.16	0.179	0.02	0.169	2.361	0.147	2.597

Simulations were carried out for a fixed Morton number ($M = 2,55.10^{-11}$) and five different Eötvös numbers varying the tube diameter. The bubbles shapes and velocity profiles for each set are shown on Fig. 4.

It can be observed in Fig. 3 the dimensionless axial velocity profiles in the three main regions of the slug flow: bubble nose, developed liquid film and wake. This qualitative result is very similar to the numerical ones obtained by Araújo *et al.* (2012) and experimental obtained by Nogueira *et al.* (2006).

The numerical dimensionless axial velocity profile (u_z/U_{TB}) are presented in Fig. 5 for different values of Eötvös numbers, the qualitative results show good agreements with the ones obtained by Araújo *et al.* (2012), in which for lower numbers of Eötvös numbers, higher is the dimensionless axial velocity.

The wall shear stresses calculated for different values of Eo is showed in Fig 6. The same behavior were presented by Araújo *et al.* (2012) for different sets of Morton and Eötvös numbers. The figure shows that the wall shear stress in the bubble wake $(0 < z/D < 1)$ reaches negative values, Araújo *et al.* (2012) explain this saying that for some distance below the bubble bottom, the liquid phase near the wall is flowing upwards, which produces stresses in the opposite direction. After this region the wall shear stress presents an short linear behavior defining where the bubble wake finishes and the bottom of the bubble begins, reaching then the region where the liquid film is stabilized. The gas bubble is small (20ml), so the stabilized liquid film region is not well defined, because of that the wall shear stress soon starts to decrease (which means the film liquid thickness starts to decrease) until it reaches the top of the bubble, where the wall shear stress becomes zero. For lower Eötvös numbers (small tube diameters) the bubble is longer, with higher values of liquid film thickness and wall shear stress as shown in Fig. 6.

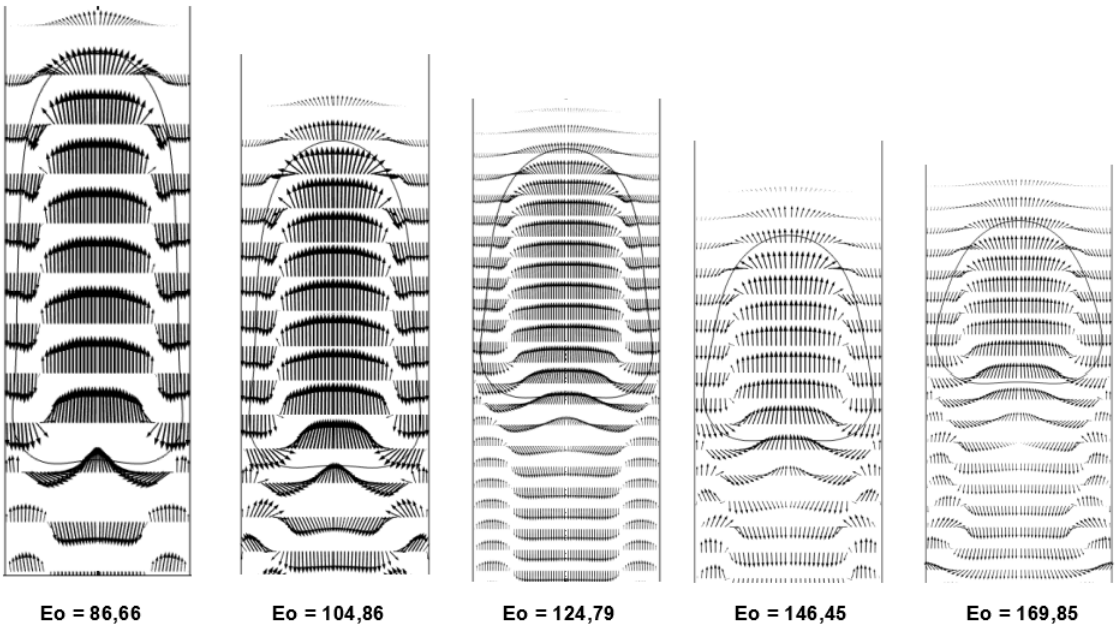

Figure 4: Bubble shapes and velocity profiles for different Eötvös numbers.

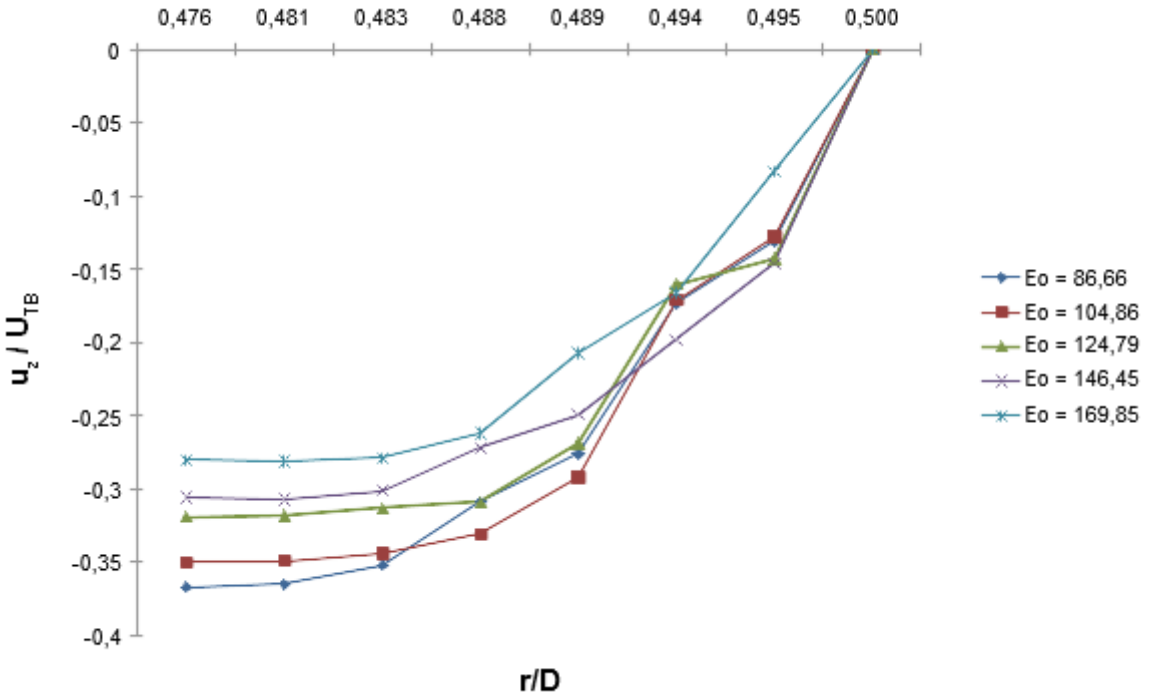

Figure 5: Numerical dimensionless axial velocity profile (u_z/U_{TB}) of 20ml bubbles on the developed liquid film region, for distinct values of Eo Araújo *et al.* (2012).

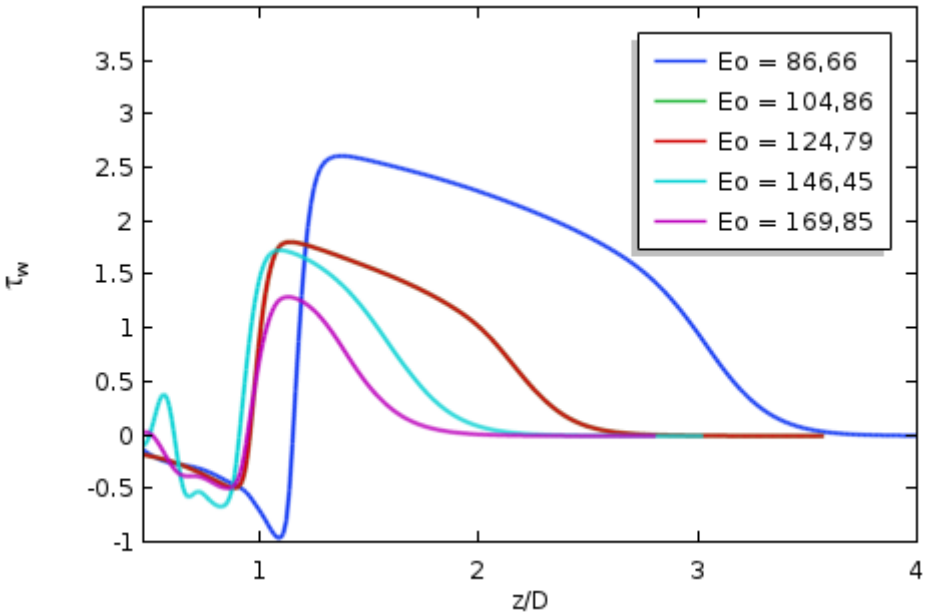

Figure 6: Wall shear stress in the axial direction in a fixed frame of reference bellow the bubble wake (τ_w) of for distinct values of Eo Araújo *et al.* (2012).

5. FINAL REMARKS

In this work, we presented the study of the flow around single Taylor bubbles rising in a vertical column of water using a non-intrusive technique, the fast film technique and by using a numerical simulation in which a phase-field method was applied. The experimental technique allowed the determination of the bubble's length and velocity, along with the liquid film thickness. A phase field model was applied to simulate flows with the same characteristics as the experimental ones and good agreement were found between numerical and experimental results. The numerical study was extended to flows with high numbers of N_f by simulating flow with different column diameters and Eötvös numbers, a particular interest was taken in the annular liquid film, where results for the dimensionless axial velocity and for the wall shear stress were presented.

6. REFERENCES

Araújo, J., Miranda, J., Pinto, A. and Campos, J., 2012. "Wide-ranging survey on the laminar flow of individual taylor bubbles rising through stagnant newtonian liquids". *International Journal of Multiphase Flow*, Vol. 43, pp. 131–148.

Brown, R., 1965. "The mecriança hanics of large gas bubbles in tubes: I. bubble felocities in stagnant liquids". *The Canadian Journal of Chemical Engineering*, Vol. 43, No. 5, pp. 217–223.

de Oliveira, W., de Paula, I., Martins, F., Farias, P. and Azevedo, L., 2015. "Bubble characterization in horizontal air–water intermittent flow". *International Journal of Multiphase Flow*, Vol. 69, pp. 18–30.

Morgado, A., Miranda, J., Araujo, J. and Campos, J., 2016. "Review on vertical gas–liquid slug flow". *International Journal of Multiphase Flow*, Vol. 85, pp. 348–368.

Nogueira, S., Riethmuler, M., Campos, J. and Pinto, A., 2006. "Flow in the nose region and annular film around a taylor bubble rising through vertical columns of stagnant and flowing newtonian liquids". *Chemical Engineering Science*, Vol. 61, No. 2, pp. 845–857.

Thome, J., Dupont, V. and Jacobi, A., 2004. "Heat transfer model for evaporation in microchannels. part i: Presentation of the model". *International Journal of Heat and Mass Transfer*, Vol. 47, No. 14-16, pp. 3375–3385. ISSN 0017-9310. doi:10.1016/j.ijheatmasstransfer.2004.01.006.

7. RESPONSIBILITY NOTICE

The following text, properly adapted to the number of authors, must be included in the last section of the paper:
The authors is are the only responsible for the printed material included in this paper.